Communication

Electrodeposition of Noble Metal Nanoparticles on Carbon Nanotubes

Bernadette M. Quinn, Cees Dekker, and Serge G. Lemay

J. Am. Chem. Soc., **2005**, 127 (17), 6146-6147• DOI: 10.1021/ja0508828 • Publication Date (Web): 05 April 2005

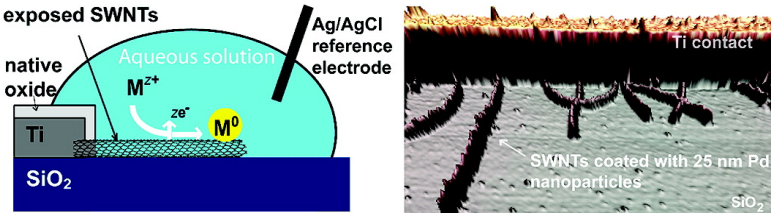

More About This Article

Additional resources and features associated with this article are available within the HTML version:

- Supporting Information
- Links to the 28 articles that cite this article, as of the time of this article download
- Access to high resolution figures
- Links to articles and content related to this article
- Copyright permission to reproduce figures and/or text from this article

View the Full Text HTML

J|A|C|S
COMMUNICATIONS

Published on Web 04/05/2005

Electrodeposition of Noble Metal Nanoparticles on Carbon Nanotubes

Bernadette M. Quinn,* Cees Dekker, and Serge G. Lemay*

Kavli Institute of Nanoscience, Delft University of Technology, Lorentzweg 1, 2628 CJ Delft, The Netherlands

Received February 10, 2005

Single-walled carbon nanotubes (SWNTs) have been proposed as the ideal metal catalyst support for electrocatalytic and sensing applications because of their unique electrical properties, high chemical stability, and high surface-to-volume ratios.[1] Methods developed to decorate nanotubes with metal nanoparticles typically involve harsh oxidative pretreatment and/or modification with surfactants, making them less useful for potential applications.[1g−k,2] Dai and co-workers recently reported the spontaneous nucleation of bare Pt and Au particles on SWNT side walls;[1f] however, the nanotube is oxidatively consumed in the process.[11] Here, we demonstrate that noble metals can be electrodeposited on SWNT sidewalls under direct potential control, where the nanotube acts as a nonsacrificial template for the deposited clusters. As the nanotube is a one-dimensional wire on an insulating substrate, metal nucleation and growth are also confined to 1D. The SWNT serves a dual function: initially as the electrodeposition template and subsequently as a wire to electrically connect the deposited Au, Pt, and Pd nanoparticles.

SWNT electrodes suitable for electrochemical measurements were produced via patterned SWNT growth following standard microfabrication techniques.[3] Briefly, catalyst islands (50 μm × 70 μm) were lithographically defined on Si/SiO_2 wafers (thermal oxide thickness 500 nm). Randomly oriented SWNTs were then grown from the catalyst using CVD.[4] Finally, Ti contact wires were patterned over the catalyst islands in a second lithographic step. The number of connected nanotubes protruding from the Ti was ca. two per micrometer. The resulting device is illustrated schematically in Figure 1a. A drop of electrolyte containing the electroactive species of interest was pipetted onto the array and an Ag/AgCl reference electrode immersed in solution. All potentials given are vs Ag/AgCl. Under ambient conditions, Ti exposed to solution is covered by a layer of native oxide that is electrochemically unreactive over a wide potential region (0−1.5 V). Cyclic voltammetry (CV) of a simple redox species, ferrocene methanol, was used to characterize the electrochemical response of the device. The steady-state wave obtained is characteristic of mass-transfer-limited electron transfer, demonstrating that the device can be considered as an array of nanoelectrodes (Supporting Information).[5]

Metal electrodeposition was performed potentiostatically in a two-electrode arrangement where the deposition potential, duration of the pulse, and the concentration of the metal salt ($HAuCl_4$, K_2PtCl_4, $(NH_4)_2PdCl_4$) were varied. Spontaneous metal deposition[1f] was *never* observed in aqueous solution without added ethanol. Tapping mode AFM (Nanoscope IIIa) was used to characterize the resulting metal deposited on the SWNT side wall. A typical CV recorded at the SWNT array in the presence of $AuCl_4^-$ is given in Figure 1b. The cathodic steady-state wave is ascribed to the reduction of Au^{3+} to Au^0 at the SWNT side walls.[6] Metal nucleation was confirmed by the appearance of an anodic stripping peak when the potential was reversed.[6] In the same figure, the CV for an identical Ti electrode without the SWNT array demonstrates that the response is due to the SWNTs.[7]

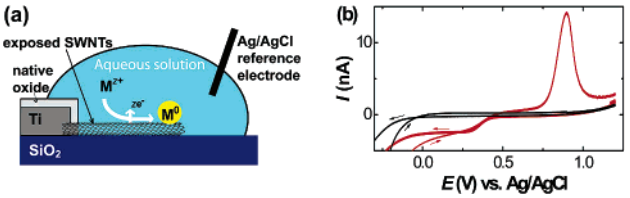

Figure 1. (a) Schematic illustration of the SWNT electrode. (b) CV response of the SWNT electrode (red line) in the presence of 0.2 mM $HAuCl_4$ and 100 mM KCl showing a reduction wave and stripping peak in the negative and positive scan directions, respectively. The response from an identical Ti/native oxide electrode without the SWNTs is also shown (black line).[7] Scan rate 100 mV s^{-1}. Arrows denote scan direction.

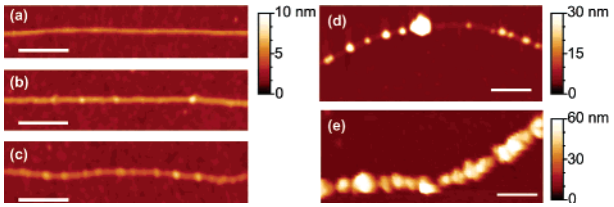

Figure 2. AFM images obtained in air pre (a) and post Au deposition at varying nucleation potentials: (b) 0.2, (c) −0.2, (d) −0.4, and (e) −0.8 V vs Ag/AgCl at separate nominally identical SWNT electrode devices. Deposition time was 20 s. Scale bar = 300 nm.

To probe the effect of nucleation potential E_n on deposition, a series of measurements was conducted on simultaneously fabricated devices where the applied nucleation voltage pulse was made progressively more negative while the duration of the pulse remained constant. Postdeposition, the device was rinsed well with water and blown dry with nitrogen, and AFM images were obtained in air for each SWNT array. The adhesion between the gold clusters and the $SWNT/SiO_2$ surface is sufficient to survive the washing and drying process. Representative images are given in Figure 2. Small clusters (height ≈ 6 nm) are apparent on the tube side walls at low coverage for $E_n = 0.2$ V. The size of the clusters and the coverage increase significantly as the potential is made more negative and at $E_n = -0.8$ V, the nanotube sidewall is almost uniformly covered by nanoparticles with an average height of 60−90 nm. For a given nucleation potential, the particle size deposited increased with both deposition time and the metal salt concentration (data not shown). The atoms cluster rather than forming a continuous monolayer, behavior that is typical of surfaces with low coordination and interfacial energies.[6,8] This experiment demonstrates that the particle size and surface coverage can be controlled by the applied potential. On 2D surfaces, electrodeposition of uniformly sized particles is hindered by the interdiffusional coupling between particles that tends to broaden the size distribution.[6] In our case, the geometry has been restricted to 1D, and under conditions where instantaneous nucleation and diffusion-controlled growth dominate (sufficiently negative potential pulse),[6,9] we do indeed observe the formation of reasonably uniform nanoparticles on the SWNT side walls. CVs recorded for the metal-decorated

10.1021/ja0508828 CCC: $30.25

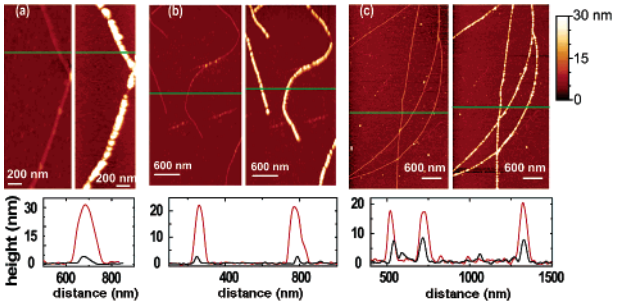

Figure 3. Tapping mode AFM images in aqueous plating solution pre and post metal deposition for (a) Au (0.2 mM $HAuCl_4$, $E_n = -1$ V, $t = 10$ s), (b) Pt (0.2 mM K_2PtCl_4, $E_n = -1$ V, $t = 10$ s), and (c) Pd (0.2 mM $(NH_4)_2PdCl_4$, $E_n = -1$ V, $t = 1$ s) with 100 mM KCl as the supporting electrolyte. Corresponding line scans pre and (black) post deposition (red) of the same position (marked with a green line in the AFM images).

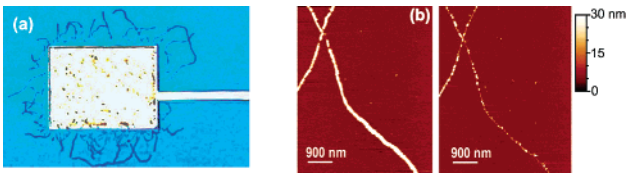

Figure 4. (a) Optical microscope images of a Ti electrode (50 μm × 70 μm) contacting nanotubes coated with Au nanoparticles of ca. 30 nm average height on an SiO_2 substrate. (b) AFM images of an Au nanoparticle plated sidewall pre (left-hand side) and post application of an oxidation pulse to the SWNT electrode (1.2 V for 600 s) in 100 mM KCl.

SWNTs were characteristic of the deposited metal (Supporting Information), demonstrating that the nanoparticles are electrically connected. Thus while the deposited metal particles do not necessarily form a continuous wire, the underlying nanotube electrically contacts all deposited clusters.

The electrodeposition process can be monitored in situ by repeating the experiments in a liquid cell in the head of the AFM. Conditions were chosen to obtain uniformly sized nanoparticles on the side walls. The corresponding images obtained in the plating solution prior to the application of a nucleation potential to the SWNT array are given in Figure 3. As can be seen from the left-hand-side images (a−c), the nanotube side walls are clean and uniform with no evidence of spontaneous nucleation for Au, Pt, and Pd. In contrast, after the application of a potential step to a region where the metal salt is reduced to zerovalent metal, the side walls are covered with a dense network of uniformly sized metal nanoparticles. As can be seen from the images, deposition occurs *solely* on the SWNTs.

For Au deposition under the conditions used in Figure 3a, the plated nanotubes were visible under an optical microscope as soon as the nucleation potential was applied (Figure 4a). This effect was not observed for Pt and Pd deposition. The wires appeared blue, consistent with the optical response of nanometer-sized gold particles where dielectric coupling between the particles red shifts the surface plasmon absorption for Au.[10] The application of a potential in the stripping regime ($E = 1.2$ V) leads to the gradual disappearance of the blue wires from the image. Post-stripping AFM images reveal the gradual dissolution of the nanoparticles from the SWNT sidewalls, as illustrated in Figure 4b where pre- and post-stripping images are given. After 600 s of stripping, some clusters remain on the sidewalls. Stripping of Pt was comparable to Au, whereas Pd was not stripped under the same conditions ($E = 1.2$ V). The reason for the latter remains unclear.

Depending on the chirality, individual SWNTs are either metallic or semiconducting.[1a] Under normal CVD growth conditions, only one in three nanotubes is metallic.[1a] As we did not observe two distinct metal particle size distributions on the SWNT arrays, both metallic and semiconducting tubes were plated equally under the conditions employed.

Nanotube side walls are generally believed to be less reactive than tube ends, with the former being compared to basal plane graphite and the latter to edge plane.[11] Under the experimental conditions employed here, sidewalls and ends were plated equally. Anodic activation of the nanotubes to introduce carboxyl functionalities to the ends and defects along the sidewalls[11b] prior to electrodeposition did not give a preference for the ends or a wider distribution of particle sizes along the side walls. In addition, we noted that nanotubes not in direct contact with Ti but contacted indirectly via nanotubes were also plated equally well (Supporting Information). This indicates that the nanotube−nanotube junction potential is not a significance source of potential loss.[12]

The key observations reported here are that metal clusters can be deposited on SWNT sidewalls under potential control. The particle size and surface coverage can be tuned with potential, deposition time, and metal salt concentration. This method offers an elegant route to growing and wiring metal nanoparticles.

Acknowledgment. Valuable discussion with Jing Kong and Iddo Heller is gratefully acknowledged. AFM images processed with WSxM; http://www.nanotec.es. This research was funded by FOM and NWO.

Supporting Information Available: Additional CVs and AFM images. This material is available free of charge via the Internet at http://pubs.acs.org.

References

(1) (a) Dai, H. *Acc. Chem. Res.* **2002**, *35*, 1035. (b) Zhang, Y.; Dai, H. *App. Phys. Lett.* **2000**, *77*, 3015. (c) Zhang, Y.; Franklin, N. W.; Chen, R. J.; Dai, H. *Chem. Phys. Lett.* **2000**, *331*, 35. (d) Guo, D.-J.; Li, H.-L. *J. Electroanal. Chem.* **2004**, *573*, 197. (e) Kong, J.; Chapline, M. G.; Dai, H. *Adv. Mater.* **2001**, *13*, 1384. (f) Choi, H. C.; Shim, M.; Bangsaruntip, S.; Dai, H. *J. Am. Chem. Soc.* **2002**, *124*, 9058. (g) Girishkumar, G.; Vinodgopal, K.; Kamat, P. V. *J. Phys. Chem. B* **2004**, *108*, 19960. (h) Hrapovic, S.; Liu, Y.; Male, K. B.; Luong, J. H. T. *Anal. Chem.***2004**, *76*, 1083. (i) Unger, E.; Duesberg, G. S.; Liebau, M.; Graham, A. P.; Seidel, R.; Kreupl, F.; Hoenlein, W. *Appl. Phys. A* **2003**, *77*, 735. (j) Xing, Y. *J. Phys. Chem. B* **2004**, *108*, 19255. (k) Serp, P.; Corrias, M.; Kalck, P. *Appl. Catal., A* **2003**, *253*, 337. (l) Song, J. H.; Yiying, W.; Messer, B.; Kind, H.; Yang, P. *J. Am. Chem. Soc.* **2001**, *123*, 10397.

(2) Zoval, J. V.; Lee, J.; Gorer, S.; Penner, R. M. *J. Phys. Chem. B* **1998**, *102*, 1166.

(3) Heller, I.; Kong, J.; Heering, H. A.; Williams, K. A.; Lemay, S. G.; Dekker: C. *Nano Lett.* **2005**, *5*, 137.

(4) (a) Kong, J.; Soh, H. T.; Cassell, A. M.; Quate, C. F.; Dai, H. J. *Nature* **1998**, *395*, 878. (b) Some ropes are also formed during CVD growth. Deposition on ropes and on individual SWNTs was comparable.

(5) Day, T. M.; Wilson, N. R.; Macpherson, J. V. *J. Am. Chem. Soc.* **2004**, *126*, 16724.

(6) Penner, R. M. *J. Phys. Chem. B* **2002**, *106*, 3339.

(7) Native Ti oxide layer breakdown occurs at $E < 0$ V, but there was no evidence of metal deposition on the underlying Ti under our experimental conditions.

(8) Zoval, J. V.; Stiger, R. M.; Biernacki, P. R.; Penner, R. M. *J. Phys. Chem.* **1996**, *100*, 837.

(9) Chen, S.; Kucernak, A. *J. Phys. Chem. B* **2003**, *107*, 8392.

(10) Ung, T.; Liz-Marzan, L. M.; Mulvaney, P. *J. Phys. Chem. B* **2001**, *105*, 3441.

(11) (a) Banks, C. E.; Moore, R. R.; Davies, T. J.; Compton, R. G. *Chem. Commun.* **2004**, *2004*, 1804. (b) Musameh, M.; Lawrence, N. S.; Wang, J. *Electrochem. Commun.* **2005**, *7*, 14.

(12) Stadermann, M. et al. *Phys. Rev. B* **2004**, *69*, 201402.

JA0508828